

Supporting Information

Promoting Angiogenesis in Oxidative Diabetic Wound Microenvironment using a Nanozyme-Reinforced Self-Protecting Hydrogel

Haibin Wu^{†,¶}, Fangyuan Li^{†,‡,¶}, Wei Shao[†], Jianqing Gao^{,†,§}, Daishun Ling^{*,†,‡,⊥}*

[†]Institute of Pharmaceutics, College of Pharmaceutical Sciences, Zhejiang University, Hangzhou 310058, P. R. China.

[‡]Hangzhou Institute of Innovative Medicine, College of Pharmaceutical Sciences, Zhejiang University, Hangzhou 310012, P. R. China.

[§]Dr. Li Dak Sum & Yip Yio Chin Center for Stem Cell and Regenerative Medicine, Zhejiang University, Hangzhou 310058, P. R. China.

[⊥]Key Laboratory of Biomedical Engineering of the Ministry of Education, College of Biomedical Engineering & Instrument Science, Zhejiang University, Hangzhou 310027, P. R. China.

Corresponding Author

*E-mail: lingds@zju.edu.cn (D. Ling), ORCID: 0000-0002-9977-0237 (D. Ling);

*E-mail: gaojianqing@zju.edu.cn (J. Gao)

Table of Contents

S1. Supplementary Methods

- S1.1 Materials and reagents
- S1.2 Preparation of PEI_{25k} functionalized ceria nanoclusters (PCNs)
- S1.3 Formation and characterization of PCN-miR complex
- S1.4 Fabrication and characterization of PCN-miR/Col hydrogel
- S1.5 Susceptibility of the collagen-based hydrogels to oxidative damage
- S1.6 Cell culture
- S1.7 *In vitro* cytotoxicity
- S1.8 Internalization of PCN-miR
- S1.9 Effect of collagen-based hydrogels on cellular fate under oxidative stress
- S1.10 Surgical excisional wounds in STZ-induced diabetic rats and treatments.
- S1.11 Histology and immunofluorescence staining of wound tissues
- S1.12 miR-26a fluorescent *in situ* hybridization
- S1.13 Photoacoustic imaging of wound tissues
- S1.14 Ultrastructural analysis of collagen deposition
- S1.15 Statistical analyses
- S1.16 Safety statement

S2. Supplementary Figures

- Figure S1. Characterization of ceria nanozymes and PCN-miR.
- Figure S2. Characterization of various collagen-based hydrogels.
- Figure S3. Biocompatibility and cellular uptake.
- Figure S4. *In vitro* ROS-scavenging capacity of the collagen-based hydrogels.

Figure S5. Immunofluorescence of intact diabetic and non-diabetic skins.

Figure S6. Characterization of wound surfaces.

Figure S7. Representative SEM images of the ultrastructure of collagen fibres.

Figure S8. Wound tissues stained with Picrosirius red.

Figure S9. Characterization of collagen in wounded tissues and intact skins.

Figure S10. Systemic toxicity evaluation.

S1. Supplementary Methods

S1.1 Materials and reagents

Branched PEI_{25k} was obtained from Sigma-Aldrich (St Louis, MO, USA). Hydrogen peroxide (H₂O₂, 30 wt%), N,N-dimethylformamide (DMF, 99.9%), genipin, and streptozotocin (STZ) were purchased from Aladdin Reagent (Shanghai, China). Cell culture medium Dulbecco's modified Eagle's medium (DMEM), fetal bovine serum (FBS), trypsin, penicillin, and streptomycin were obtained from Gibco BRL (Gaithersburg, USA). AntagomiR-26a, Cy5-labeled antagomiR-26a, and scrambled miRNA were synthesized by Sangon Biotech Co. Ltd. (Shanghai, China). CellTiter 96 AQueous One Solution Cell Proliferation Assay kit (MTS) was purchased from Promega (Madison, WI, USA). ROS assay kit (DCF-DA), senescence-associated β -galactosidase (SA- β -gal) staining kit, and lipid peroxidation MDA assay kit were purchased from Beyotime Institute of Biotechnology (Haimen, China). Rat tail type I collagen, Calcein-AM/PI double staining, and JC-1 Mitochondrial Membrane Potential Assay Kit were purchased from Yeasen biotech Co. Ltd. (Shanghai, China). Protein carbonyl assay kit was obtained from Nanjing Jiancheng Bioengineering Institute (Nanjing, China). All chemicals and reagents were used as received without further purification.

S1.2 Preparation of PEI_{25k} functionalized ceria nanoclusters (PCNs)

2-Bromo-2-methylpropionic acid (BMPA)-capped ceria nanozymes used in this study were synthesized according to a previously reported procedure.^{1,2} The as-obtained BMPA-capped ceria nanozymes were dispersed in N,N-dimethylformamide (DMF) for

next steps. In a typical procedure, 1 ml of PEI_{25k} DMF solution (80 mg mL⁻¹) was dropped swiftly to 5 mL of BMPA-capped ceria nanozymes dispersion (3 mg mL⁻¹). The mixture was then stirred for 3 hours at room temperature. The PCN was collected by centrifugation, washed with ethanol and deionized water for several times respectively, and dispersed in deionized water for further use.

S1.3 Formation and characterization of PCN-miR complex

For the preparation of PCN-miR complex, predetermined amounts of PCNs and antagomiR-26a were separately dissolved in phosphate buffered saline (PBS) with different N:P ratios. Equal volume of the two solutions were mixed by vortex and then kept stand for 30 minutes to fully enable miRNA complexation. DLS size and surface charge of the antagomiR-26a alone or PCN-miR complex at various N:P ratios (5, 10, 20, and 40) were measured using a Zetasizer Nano ZS90 equipment (Malvern instruments, UK) at 25 °C. To verify miRNA complexation ability of the PCNs, agarose gel electrophoresis was performed on a PowerPac™ Basic electrophoresis apparatus (Bio-Rad Laboratories Inc., USA). Typically, solutions (20 μL) of PCN-miR at various N:P ratios (0, 1.25, 2.5, 5, 10, 20, and 40) were diluted with 4 μL of 6× agarose gel loading buffer. The mixtures were then loaded onto the 2.5% agarose gels stained with GelRed (1:10000 v/v) and ran with 1× Tris-borate-EDTA (TBE) buffer at 120 V for 40 min. The motion retardation of miRNA was visualized by using the G:BOX BioImaging System (Syngene).

S1.4 Fabrication and characterization of PCN-miR/Col hydrogel

The PCN-miR/Col hydrogel was fabricated by crosslinking with genipin according to

a previously reported protocol.³ Briefly, the PCN-miR complex (N:P ratio, 10), 1N NaOH, and soluble rat tail type I collagen were combined in PBS and vortexed for 10 s. The gelation process was then initiated by adding genipin solution to the pre-gel solution with a final concentration of type I collagen at 2 mg/mL, genipin at 1 mM. The mixture solution was incubated at 37 °C for another 3 hours to achieve hydrogel gelation. After the gelation process, the uncrosslinked agents were removed by rinsing the hydrogel in PBS solution. miR/Col and P-miR/Col hydrogels were also prepared at the same condition except that the polycation PEI_{25k} was not functionalized with ceria nanozymes.

Turbidimetric gelation kinetics of collagen-based hydrogels with various formulations were determined. Pre-gel mixtures were added (50 µL/well) into a 96 well plate and the absorbance at 313 nm was recorded every 60 seconds using an Infinite M1000Pro microplate reader (Tecan, USA) preheated to 37 °C. The TEM and STEM-EDX morphological and element distribution characteristics of the PCN-miR were characterized using a FEI Tecnai F20 at a voltage of 200 kV. Distribution of phosphorus element, as a characteristic element in the nucleic acid miRNAs, and nitrogen element in the PEI_{25k} were investigated for the characterization of PCN-miR nanocomplexes. To characterize the distribution of miRNAs in hydrogels, collagen-based hydrogels were prepared using Cy5-labeled antagomiR-26a and Fluorescein isothiocyanate - labelled collagen. After air-drying, the fluorescent collagen-based hydrogels were visualized on a Nikon A1R confocal microscope (Nikon, Japan). The surface microstructure and elemental composition of the collagen-based hydrogels were further assessed by a Hitachi SU8010 field emission SEM equipped with an EDX spectrometer and a Veeco Dimension-ICON atomic force microscope.

S1.5 Susceptibility of the collagen-based hydrogels to oxidative damage

To assess the resistance of hydrogels to oxidative damage, the collagen-based hydrogels were examined with XPS and Raman tests before and after exposure to 1M H₂O₂ for 12 hours. The Raman mapping of the collagen-based hydrogels before and after H₂O₂ treatment were recorded using a Horiba LabRAM HR Evolution Raman system equipped with a 532 nm laser (Horiba Scientific, Japan). XPS spectra of the collagen-based hydrogels before and after H₂O₂ exposure were obtained on an ESCALAB 250XI photoelectron spectrometer (ThermoFisher Scientific, USA). Binding energies in the high resolution XPS spectra were referenced to the *C1s* binding energy of 284.6 eV. CD spectra of the collagen-based hydrogels incubation in PBS or 500 μM H₂O₂ for 12 hours were acquired on a Jasco J-1500 CD spectrometer (Jasco Inc., Japan) using a 1 mm path length quartz cuvette at room temperature. The CD spectra were obtained by averaging three measurements.

S1.6 Cell culture

The human umbilical vein endothelial cells (HUVECs) and immortalized human skin keratinocytes (HaCaTs) were acquired from Cell Institute of Chinese Academy of Sciences (Shanghai, China) and Biomics Biotechnologies Co., Ltd (Nantong, China), respectively. HUVECs were maintained under standard conditions and fed every 2 days with RPMI 1640 supplemented with 10% (v:v) fetal bovine serum and 1% (v:v) penicillin/streptomycin. HaCaTs were cultured under standard conditions and fed every 2 days with Dulbecco's modified Eagle's Medium (DMEM), containing 10% (v:v) fetal bovine serum and 1% (v:v) penicillin/streptomycin.

S1.7 In vitro cytotoxicity

HUVECs were seeded into a 96-well plate and cultured for 24 hours (1×10^4 cells/well). The cells were subsequently incubated with PCNs, PEI_{25k}, or PCN-miR complex at various concentrations or N:P ratios for 24 hours. An MTS cell proliferation assay was conducted using the CellTiter 96 Aqueous One Solution Cell Proliferation Assay according to the manufacturer's instructions. Typically, 20 μ L of CellTiter 96 Aqueous One Solution reagent was added into each well and incubated at 37 °C for 3 hours. Absorbance at 490 nm was recorded via the Elx-800 microplate reader (Bio-Tek Instruments, USA). Relative cell viability was expressed as a fraction of the absorbance from the control wells incubated with cell culture medium, which was set to 100%. Furthermore, Calcein-AM/PI double staining kit was used to evaluate the viability of HaCaT and HUVEC seeded on collagen-based hydrogels for 96 hours according to the manufacturer's instructions. Fluorescence images were acquired using a Nikon A1R confocal microscope (Nikon, Japan).

S1.8 Internalization of PCN-miR

To track the cellular uptake of antagomiR-26a, Cy5-labelled antagomiR-26a was used for the complexation. A 35 mm confocal glass-bottom dishes (NEST, Shanghai, China) was seeded with HUVECs (1×10^5 cells/well), and the cells were grown for 24 hours prior to incubation of naked antagomiR-26a or PCN-miR complex (1 μ g miRNA/dish, N:P ratio = 10) for 6 hours. The nucleus and lysosomes were stained with 4',6-diamidino-2-phenylindole (DAPI) and LysoTracker green DND-26, respectively.

Fluorescence images of cells were captured with a Nikon A1R confocal microscope (Nikon, Japan).

S1.9 Effect of collagen-based hydrogels on cellular fate under oxidative stress

HUVECs were seeded (1×10^5 cells/well) into a 35 mm confocal glass-bottom dishes pre-coated with collagen-based hydrogels (1 μ g miRNA/dish, N:P ratio = 10). After culture for 48 hours, culture media was replaced with 500 μ M of H_2O_2 for 2 hours prior to the Calcein-AM/PI double staining (cell survival), DCF-DA staining (ROS measurement), or JC-1 (mitochondrial membrane potential) staining according to the manufacturer's protocols. For monitoring the extent of H_2O_2 induced DNA damage, cells treated as described above were grown for another 24 hours prior to the γ -H2AX labelling (double-stranded DNA breaks). Briefly, cells were washed with ice-cold PBS and fixed with 4% paraformaldehyde. After treated with blocking buffer, cells were then incubated with primary γ -H2AX rabbit monoclonal antibodies (Beyotime Institute of Biotechnology, AF1201), subsequently with Alexa Fluor 647-labeled secondary antibodies (Beyotime Institute of Biotechnology, A0468), and the cell nucleus were counterstained with DAPI. Fluorescence images of the stained cells were obtained with a Nikon A1R confocal microscope (Nikon, Japan), and the acquired confocal images were analysed using the ImageJ software (NIH, Bethesda, MD).

For the lipid peroxidation and protein carbonylation assays, the levels of malondialdehyde (a product of lipid peroxidation) and carbonylated proteins in the lysates of cells treated as described above were quantified by the lipid peroxidation MDA assay kit and the protein carbonyl assay kit, respectively, according to the manufacturer's recommended procedures.

For flow cytometric analysis of cellular ROS level, HUVECs were seeded into a 6-well plate (2×10^5 cells/well) pre-coated with collagen-based hydrogels (1 μ g miRNA/dish, N:P ratio = 10) and grown for 48 hours. Cells were washed and incubated in fresh culture media containing 500 μ M of H₂O₂ for 2 hours prior to the DCF-DA staining. Cells were then rinsed with PBS, and the DCF signal was recorded by a BD Accuri C6 Flow Cytometer (BD Biosciences, CA). Data analysis was performed with the FlowJo software.

In the senescence assay, HUVECs were seeded into a 12-well plate (5×10^4 cells/well) pre-coated with collagen-based hydrogels (1 μ g miRNA/dish, N:P ratio = 10) and grown for 48 hours. Cells were washed and incubated in fresh culture media containing 500 μ M of H₂O₂ for 2 hours. After culturing for four days, the cells were stained for SA- β -gal activity using a SA- β -gal staining kit according to the manufacturer's protocols.

S1.10 Surgical excisional wounds in STZ-induced diabetic rats and treatments

All *in vivo* experimental procedures were conducted under approval from the Animal Experimental Ethics Committee of Zhejiang University. Male Sprague–Dawley (SD) rats weighing about 200g were purchased from Shanghai SLAC Laboratory Animal Co. Ltd. (Shanghai, China). Diabetic rat models were induced by intraperitoneal administration of STZ (70 mg/kg body weight) dissolved in pH 4.5 citrate buffer. Rats with blood glucose levels >16.7 mmol/L were defined as diabetic and maintained for another 4 weeks prior to wound induction. For the creation of surgical excisional wounds, STZ-induced diabetic rats were anesthetized with 1% sodium pentobarbital solution (40 mg/kg body weight, intraperitoneally). The dorsal hairs of the diabetic rats were subsequently shaved, and full-thickness excision (15 mm in diameter) was created

on the dorsal surface. Next, the wounded diabetic rats were randomly assigned to six groups (n = 5): blank control (50 μ L PBS buffer); Col (50 μ L Col hydrogel); P-miR/Col (50 μ L P-miR/Col hydrogel); PCN/Col (50 μ L PCN/Col hydrogel); PCN-scR/Col (50 μ L PCN-scR/Col hydrogel); PCN-miR/Col (50 μ L PCN-miR/Col hydrogel). Photographs of the treated wounds were recorded every 2 days by a digital camera (Nikon) with a ruler by the side of wound and then analysed by using the ImageJ software to calculate the wound area.

S1.11 Histology and immunofluorescence staining of wound tissues

Wound tissues were harvested from rats in each group at day 28 post-wounding and fixed with 4% paraformaldehyde. The fixed wound tissues were subsequently embedded in paraffin and sections of 3-4 μ m thickness were prepared. Following deparaffination and rehydration, the wound sections were then stained with Masson's trichrome, Picrosirius red for histological analysis. Besides, for systemic toxicity evaluation, the major organs including heart, liver, spleen, lung, and kidney from each treatment group at day 28 post-wounding were harvested and stained with hematoxylin and eosin (H&E). For immunofluorescence evaluations, deparaffinised and rehydrated sections of treated wound tissues were further incubated with anti-8-OHdG (Bioss Antibodies, bs-1278R), anti-4-HNE (Bioss Antibodies, bs-6313R), anti-CD68 (Abcam, ab955), anti-CD31 (Abcam, ab28364), anti-VEGF (Abcam, ab46154), or anti-Ki67 (Abcam, ab16667) antibodies, followed by incubation with the corresponding fluorescence-labelled secondary antibodies (Invitrogen/Dawen Biotec) and cell nuclear staining with DAPI. The histological sections and immunofluorescence sections were imaged within the newly formed granulation tissue by a Nikon Eclipse Ti-S microscope

(Nikon, Japan) and a Nikon A1R confocal microscope (Nikon, Japan), respectively. Fluorescence intensities of the stained markers were quantified by using the ImageJ software (NIH, Bethesda, MD) and normalized to DAPI-stained nuclei counts.

S1.12 miR-26a fluorescent in situ hybridization

Fluorescent *in situ* hybridization (FISH) was conducted with FAM-labelled miRNA probes (TSINGKE, Beijing, China) for detecting miR-26a in wound tissues. Probe hybridization was conducted using the reagents and protocols from the manufacturer (Servicebio, Wuhan, China). Wound tissues were firstly fixed by adding 4% paraformaldehyde diluted with diethyl pyrocarbonate in water for 1 hour. Wound tissues were subsequently incubated with the miR-26a probe in hybridization buffer for 12 hours at 37 °C. The obtained tissues were washed, stained with DAPI, and then processed for CLSM imaging by a Nikon A1R confocal microscope (Nikon, Japan).

S1.13 Photoacoustic imaging of wound tissues

Oxygen saturation map and grey scale B-mode imaging of the wound tissues at day 28 post-wounding were acquired by using the Oxy-Hemo mode (750 and 850 nm excitation) on a Vevo 2100 LAZR system (Verasonics Inc., Toronto, Canada). Total hemoglobins and oxygenated hemoglobin percentages in the wound tissues were quantified with the Vevo software tools (HemoMeaZure™ and OxyZated™, respectively).

S1.14 Ultrastructural analysis of collagen deposition

Wound tissues from each treated group at day 28 post-wounding were fixed with 2.5% glutaraldehyde and then dehydrated in serial ethanol solutions. The tissues were

subsequently postfixes with an aqueous osmium tetroxide solution. After air-drying overnight, the fixed wound tissues were coated with a layer of gold prior to observation on a SU8010 field emission scanning electron microscope (Hitachi, Tokyo, Japan).

S1.15 Statistical analyses

All quantitative results are expressed as mean \pm sd. Statistical analysis was performed by using two-tailed unpaired Student's *t* tests. The level of statistical significance was set at $p < 0.05$ and was used throughout the present study. Statistical evaluations of experimental data were conducted using GraphPad Prism 6.0 software.

S1.16 Safety statement

No unexpected or unusually high safety hazards were encountered.

S2. Supplementary Figures

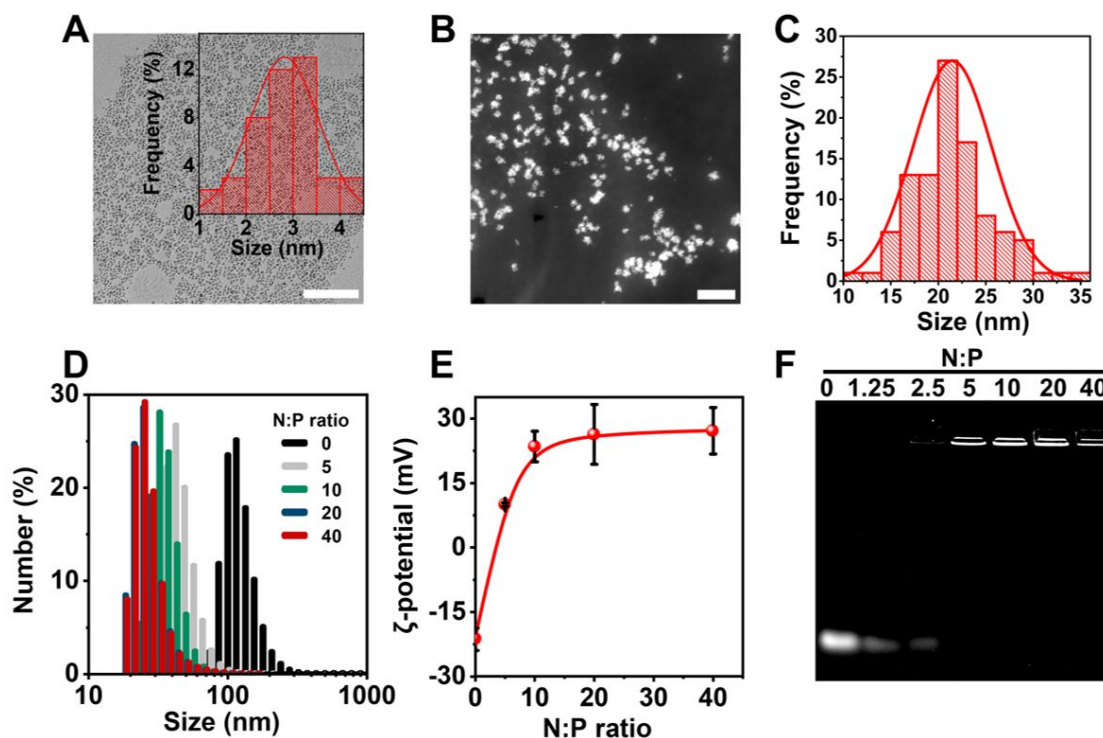


Figure S1. Characterization of ceria nanozymes and PCN-miR. (A) TEM image of ceria nanocrystals. Inset is the size distribution diagram of ceria nanocrystals as measured by Nano Measure software. Scale bar, 100 nm. (B) Scanning transmission microscopy (STEM) image of in PCN-miR. Scale bar, 100 nm. (C) Size distribution diagram of PCN-miR as measured by Nano Measure software. (D) DLS size distributions of PCN-miR at various N:P ratios. (E) ζ -potential of PCN-miR as a function of N:P ratio, $n = 3$. All data are represented as mean \pm sd. (F) A representative agarose gel electrophoresis image illustrating the complexation efficiency of antagomiR-26a with PCNs at different N:P ratios ranging from 1.25:1 to 40:1.

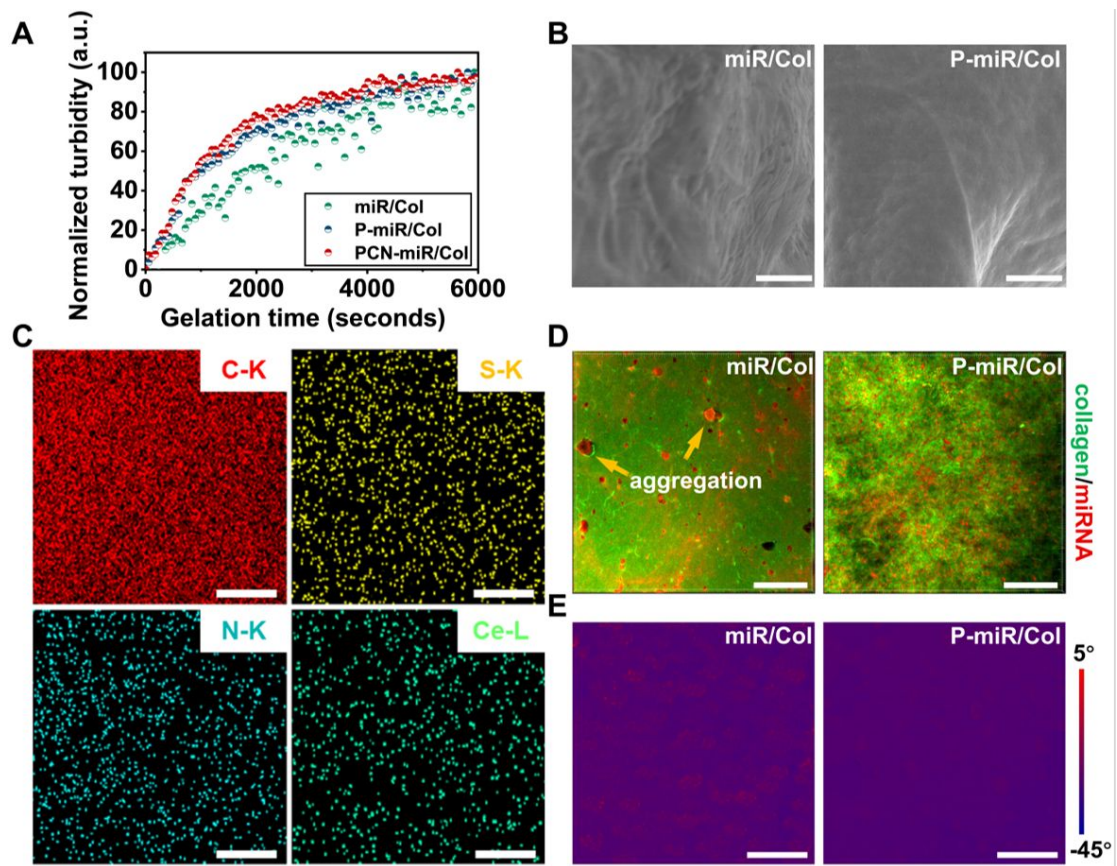


Figure S2. Characterization of various collagen-based hydrogels. (A) Turbidimetric gelation kinetics of different collagen-based hydrogels. (B) SEM images of the surface of miR/Col and P-miR/Col. Scale bars, 1 μm . (C) The EDX elemental mapping images of Ce, S, N, and C for PCN-miR/Col, which confirm the uniform distribution of PCN-miR and collagen protein in the PCN-miR/Col. Scale bars, 5 μm . (D) Three-dimensional CLSM images of miR/Col and P-miR/Col, collagen from the hydrogel is labelled with fluorescein isothiocyanate (green) and antagomiR-26a is tagged with Cy5 (red). Scale bars, 100 μm . (E) AFM phase images of miR/Col and P-miR/Col. Scale bars, 500 nm.

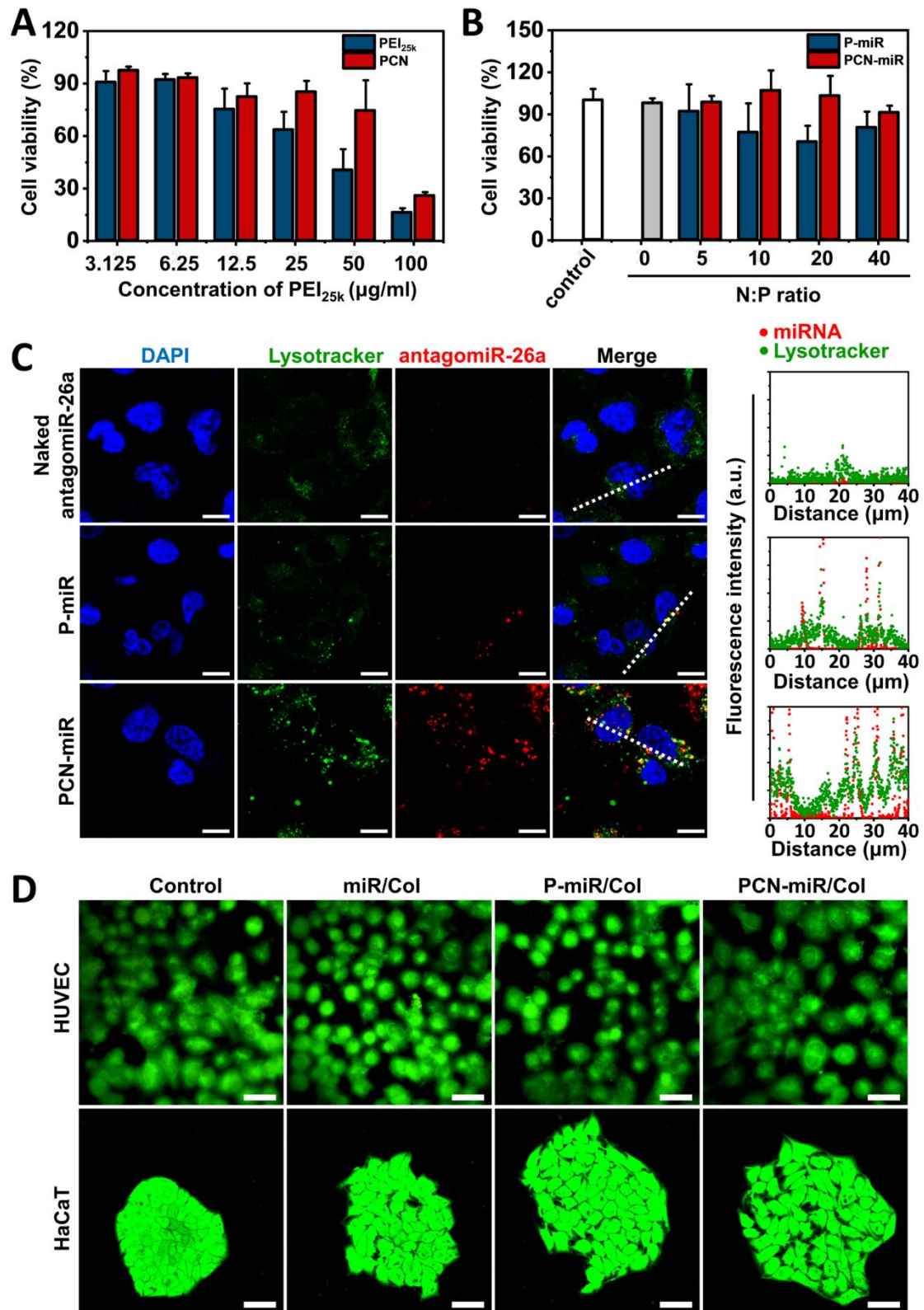


Figure S3. Biocompatibility and cellular uptake of hydrogels. (A and B) Cytotoxicity of (A) PCNs at different concentrations of PEI_{25k} and (B) PCN-miR at various N:P ratios in comparison with P-miR, $n = 4$. All data are represented as mean \pm sd. (C) Uptake of Cy5-labeled antagomiR-26a (red) into HUVECs after 6-hour incubation. Cells were co-labelled with LysoTracker Green DND-26 (green) and DAPI (blue) to track acidic organelles and nuclei, respectively. Right: Corresponding line profiles of the fluorescence signals were obtained along the white dashed lines in CLSM images,

which clearly demonstrated the co-localization of antagomiR-26a and acidic organelles. Scale bars, 10 μ m. (D) Viability was evaluated by the LIVE/DEAD assay of HUVECs and HaCaTs cultured on collagen-based hydrogels for 96 hours. Scale bars, 50 μ m.

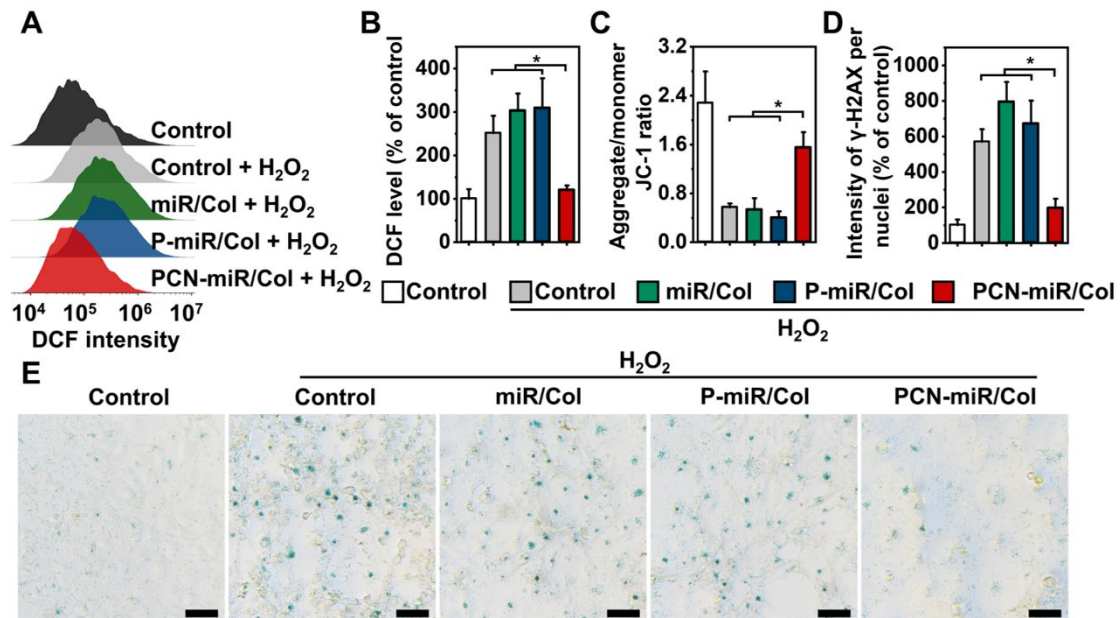


Figure S4. *In vitro* ROS-scavenging capacity of the collagen-based hydrogels. (A) Flow cytometric histograms of H₂O₂-induced intracellular ROS accumulation in HUVECs with various indicated pre-treatments, as determined by 2'-7'-dichlorodihydrofluorescein diacetate (DCF-DA) probe, which can yield the highly fluorescent 2'-7'-dichlorodihydrofluorescein (DCF) in the presence of ROS. (B) DCF levels of the H₂O₂-induced intracellular ROS accumulation in HUVECs with various indicated pre-treatments were quantitatively measured by flow cytometry (n = 3). (C) Quantitative analysis for JC-1 aggregate: monomer ratios in cells with various indicated pre-treatments after exposure to H₂O₂ (n = 4). (D) Quantification of DNA strand breaks by immunofluorescence intensity of nuclear γ -H2AX in cells with various indicated pre-treatments after exposure to H₂O₂ (n = 4). (E) Representative senescence-associated β -galactosidase (SA- β -gal) staining for H₂O₂-induced senescent phenotype in HUVECs with various indicated pre-treatments. Scale bars, 50 μ m. **P* < 0.05 by Student's *t* test. All data are represented as mean \pm sd.

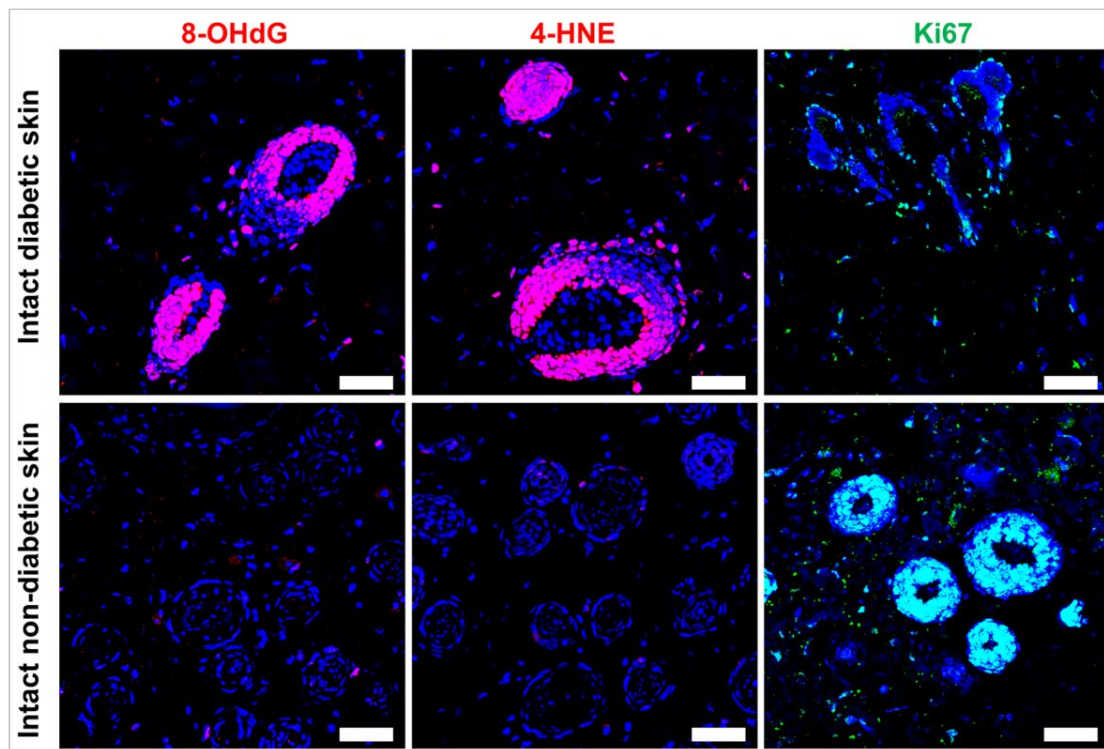


Figure S5. Immunofluorescence of intact diabetic and non-diabetic skins. Representative confocal images of immunofluorescence staining for 8-OHdG, 4-HNE, and Ki67 in intact diabetic and non-diabetic skins. Scale bars, 50 μ m.

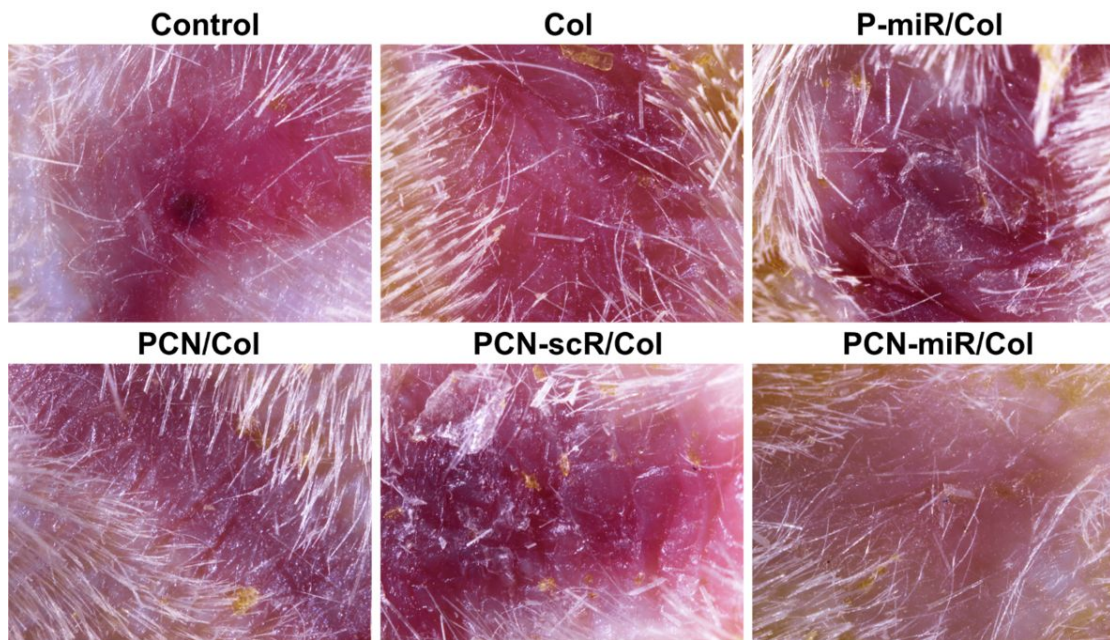


Figure S6. Characterization of wound surfaces. Wound surfaces of different treatment groups at day 28 post-wounding were visualized using a Nikon AZ100 stereomicroscope.

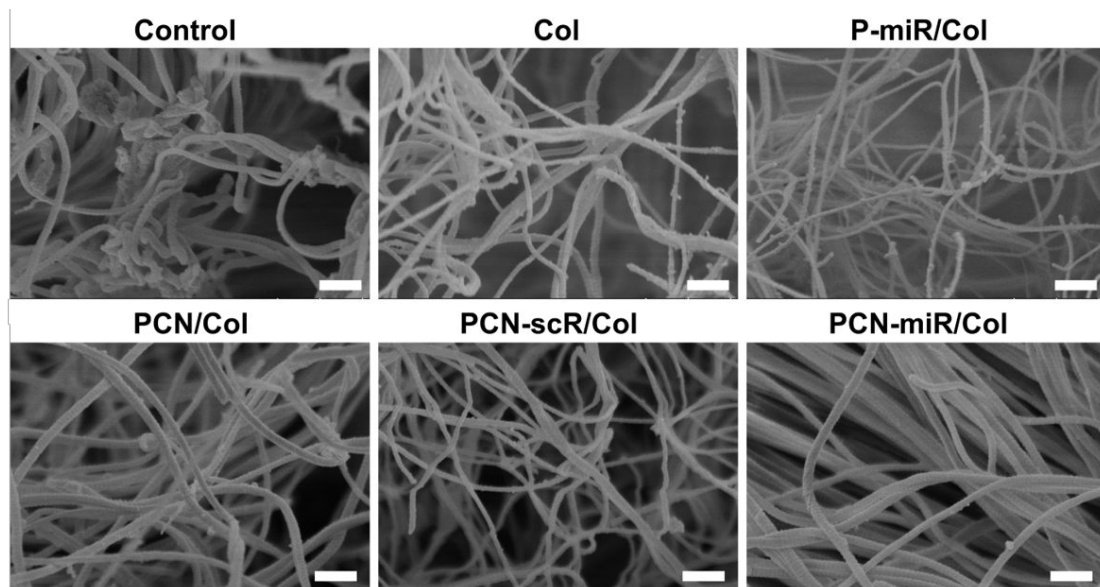


Figure S7. Representative SEM images of the ultrastructure of collagen fibres from wound tissues after 28 days of treatment. Scale bars, 500 nm.

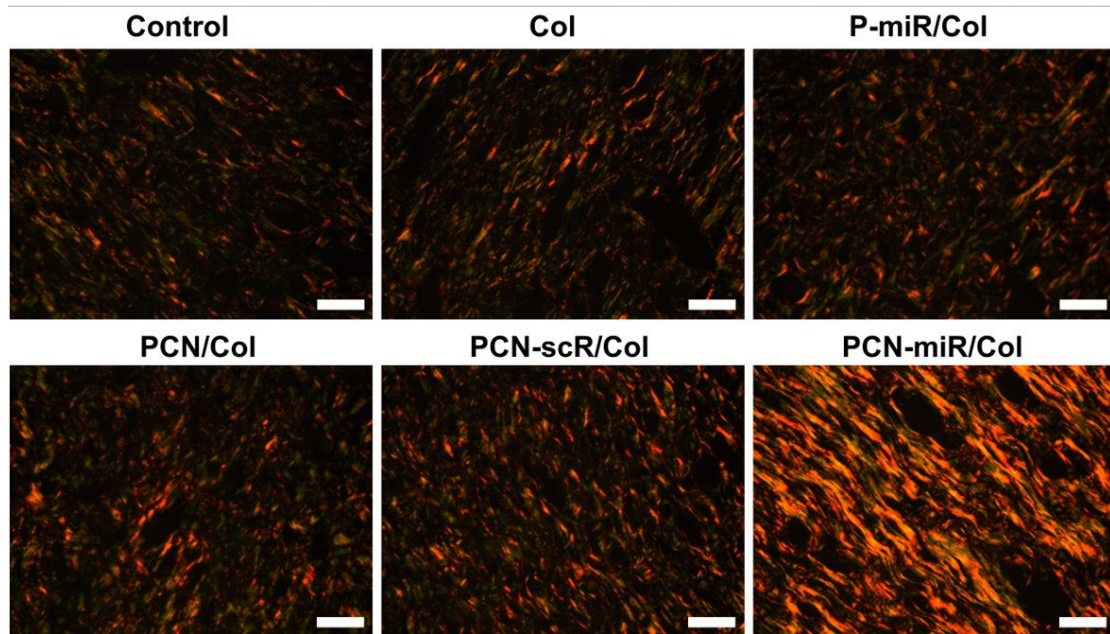


Figure S8. Wound tissues after 28 days of treatment stained with Picosirius red and imaged by polarization microscopy for detection of collagen type I (thick, yellow-orange) and collagen type III (thin, green). Scale bars, 50 μm .

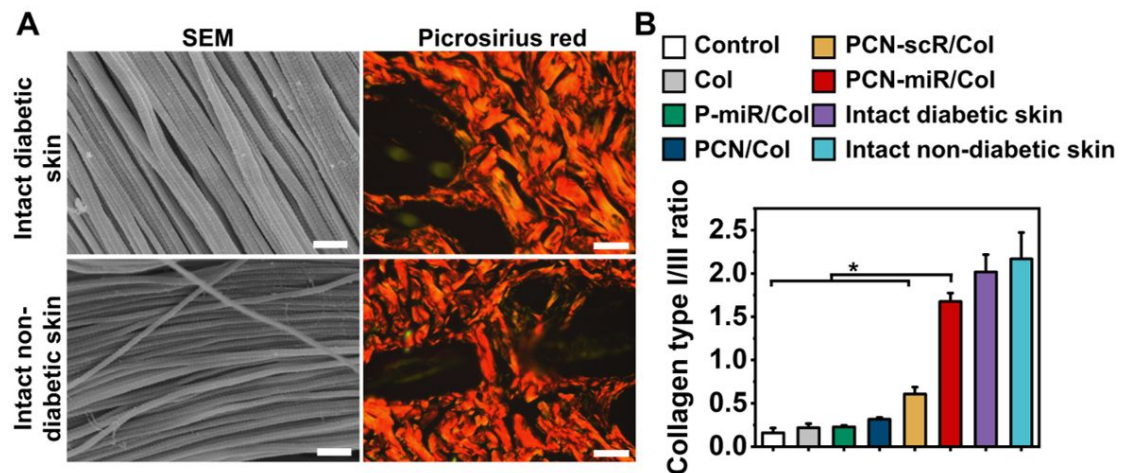


Figure S9. Characterization of collagen in wounded tissues and intact diabetic or non-diabetic skins. (A) Left column: representative SEM images of the ultrastructure of collagen fibres in intact diabetic and non-diabetic skins. Scale bars, 500 nm. Right column: intact diabetic and non-diabetic skins were stained with Picosirius red and imaged by polarization microscopy. Collagen type I (thick, yellow-orange) and collagen type III (thin, green). Scale bars, 50 μm . (B) Type I/III collagen ratios for treated wounds at day 28 post-wounding, intact diabetic skin, and intact non-diabetic skin. The ratios of type I (yellow-orange pixels) and III collagen (green pixels) in Picosirius red stained images were analysed using ImageJ software (NIH, Bethesda, MD). * $P < 0.05$ by Student's t test. All data are represented as mean \pm sd. $n = 3$.

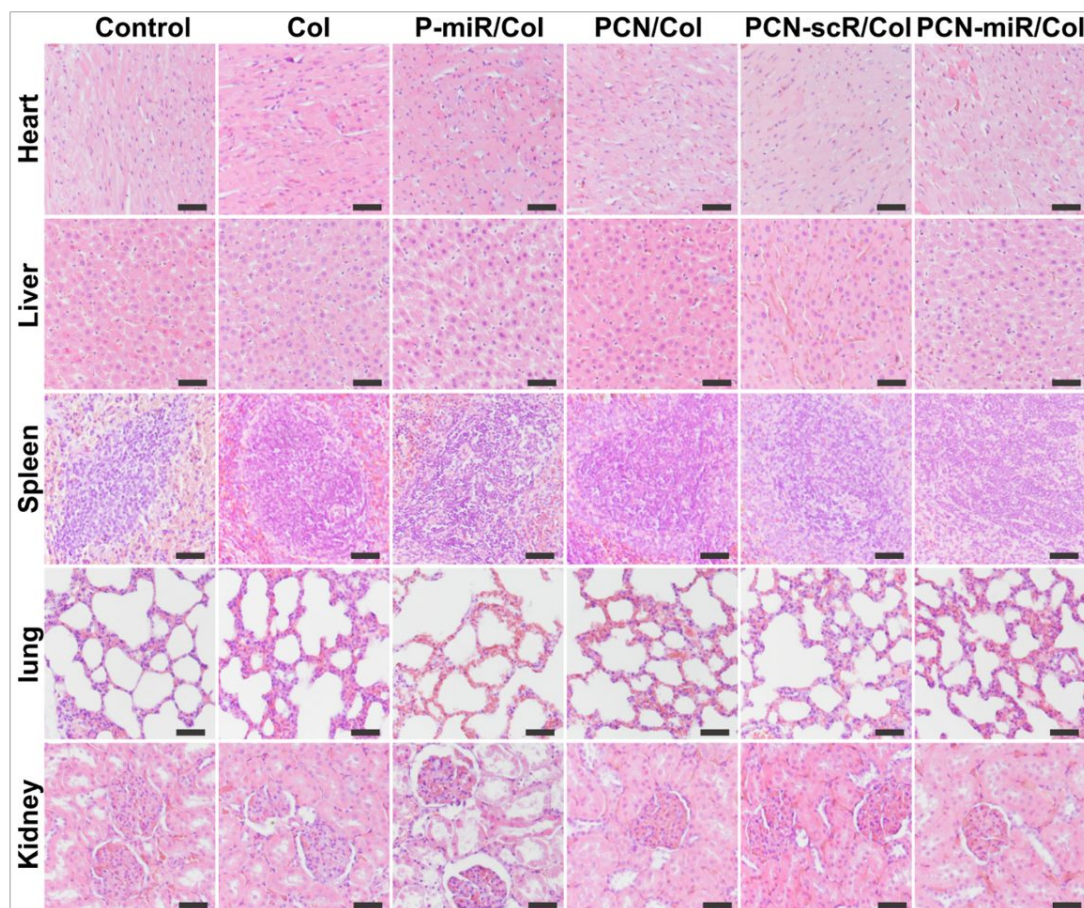


Figure S10. Systemic toxicity evaluation. Heart, liver, spleen, lung, and kidney from different treatment groups at day 28 post-wounding were collected and stained with H&E for the systemic toxicity evaluation. Scale bars, 100 μ m.

References

- (1) Kim, C. K.; Kim, T.; Choi, I. Y.; Soh, M.; Kim, D.; Kim, Y. J.; Jang, H.; Yang, H. S.; Kim, J. Y.; Park, H. K. Ceria nanoparticles that can protect against ischemic stroke. *Angew. Chem. Int. Ed.* **2012**, *51*, 11039-11043.
- (2) Wu, H.; Li, F.; Wang, S.; Lu, J.; Li, J.; Du, Y.; Sun, X.; Chen, X.; Gao, J.; Ling, D. Ceria nanocrystals decorated mesoporous silica nanoparticle based ROS-scavenging tissue adhesive for highly efficient regenerative wound healing. *Biomaterials* **2018**, *151*, 66-77.
- (3) Macaya, D.; Ng, K. K.; Spector, M. Injectable collagen-genipin gel for the treatment of spinal cord injury: in vitro studies. *Adv. Funct. Mater.* **2015**, *21*, 4788-4797.